Neutron-diffraction determination of the microscopic structure of liquid deuterium

M. Zoppi and U. Bafile
Istituto di Elettronica Quantistica, Consiglio Nazionale delle Ricerche, via Panciatichi 56/30, I-50127 Firenze, Italy

R. Magli
Dipartimento di Energetica, Università degli Studi di Firenze, via di S. Marta, I-50139 Firenze, Italy

A. K. Soper
Rutherford Appleton Laboratory, Neutron Division, Chilton, Didcot, Oxon OX11 0QX, United Kingdom
(Received 14 December 1992)

The structure factor of liquid deuterium has been measured at five points close to the triple point using time-of-flight neutron diffraction. The experiment was performed partially on the 20.7-K isotherm and partially on the 25.44-nm^{-3} isochore so that both the density derivative at constant temperature and the temperature derivative at constant density of the structure factor could be evaluated.

PACS number(s): 61.25.Em, 61.12.Gz

I. INTRODUCTION

The fundamental importance of experiments aimed at throwing light on the microscopic properties of quantum liquids, and in particular of neutron-diffraction measurements of the structural properties, has been recognized and largely exploited in the case of helium [1]. On the contrary, there is a somewhat surprising lack of neutron-diffraction data in the case of liquid hydrogen (H_2 and D_2) [2], the only experiment so far reported, to our knowledge, being the one by Ishmaev *et al.* [3].

There are, however, good reasons for investigating the structure of liquid hydrogen. The quantum behavior of a light-atomic or -molecular fluid at low temperature can be considered to arise when the delocalization of a particle, due to the spread of its wave packet and measured by the de Broglie thermal wavelength [4] $\Lambda=\hbar(2\pi/Mk_BT)^{1/2}$, becomes comparable with the size σ of the particle. Here $\hbar$ is the Planck constant divided by 2π, k_B is the Boltzmann constant, M is the particle mass, and T is the temperature. At even lower temperature, when Λ is comparable with the average interparticle distance l, the delocalization is such to allow the occurrence of exchange effects, and quantum statistics begins to play a role.

The comparison between Λ, σ, and l for some simple light liquids in the thermodynamic region between the critical and the triple point is reported in Table I. It appears that, while in helium the exchange quantum effects are always important, in hydrogen the overlap of the wave functions of two neighbor molecules is much smaller ($\Lambda/l<1$), although the spread of each wave packet is of the order of σ. In deuterium and in neon the exchange effects are very small and in the latter case even the amount of quantum diffraction is limited.

We note that in the case of liquid neon the amount of the reported experimental work in the field of neutron diffraction, though not large, is still greater than in hydrogen or deuterium [5]. Therefore, it seems that the intermediate situation, in which quantum diffraction effects are important but exchange phenomena are limited, is the least deeply studied so far. Such an intermediate case is also important because theories and simulation techniques are more easily implemented in the absence of quantum exchange, and the individual molecules can be modeled as Boltzmann particles.

One main reason for this lack of diffraction data is the role played by the so-called inelasticity effects. The way the inelastic scattering affects the diffraction pattern and how the experimental data can be corrected for it have been the subject of much work [6]. Such a correction is obviously more difficult in a molecular system than in a monatomic one. Two well-known features of the inelasticity effects on the diffraction spectra are of interest here. First, their importance increases with the scattering angle. As a consequence, in a neutron-diffraction experi-

TABLE I. Importance of quantum effects in the liquid state. Subscripts cr and tr refer to the critical and the triple point, respectively.

System	Ref.	T_{cr} (K)	T_{tr} (K)	n_{cr} (nm^{-3})	n_{tr} (nm^{-3})	$(\Lambda/\sigma)_{cr}$	$(\Lambda/\sigma)_{tr}$	$(\Lambda/l)_{cr}$	$(\Lambda/l)_{tr}$
He	[26]	5.20	2.18[a]	10.47	21.99[a]	1.50	2.31[a]	0.84	1.66[a]
H_2	[27]	33.19	13.96	9.00	23.06	0.72	1.11	0.44	0.94
D_2	[13]	38.34	18.71	10.44	25.99	0.47	0.68	0.31	0.60
Ne	[28]	44.4	24.55	14.31	37.2	0.21	0.29	0.14	0.26

[a]Relative to the λ point.

ment at a reactor source, where the variation in the exchanged momentum $\hbar Q$ is obtained by changing the scattering angle, the inelasticity appears as the typical falloff of the measured intensity as a function of Q. Second, the inelasticity effect is larger for systems composed of light molecules and, therefore, the correction procedure first introduced by Placzek [6], and usually adopted in order to correct for the above-mentioned falling off, cannot be applied to systems whose molecular mass is comparable with that of the neutron.

In this respect there is an intrinsic advantage in using time-of-flight (TOF) neutron diffraction for measuring the static structure factor $S(Q)$ of liquids composed of light molecules, which is related to the fact that here the scattering angle is kept fixed and the spread in Q is obtained simply from the energy distribution of the incident neutrons. As a matter of fact, the availability of pulsed neutron sources has made it possible to perform more accurate diffraction experiments on light fluids, and the static structure factor of deuterium gas has been measured [7].

The experiment by Ishmaev *et al.* [3], performed on both gaseous and liquid ortho-deuterium, gave results which were unphysical at low Q and inconsistent with the determination of Ref. [7]. A possible source of error could have been the use of an average over all the diffraction patterns measured by 14 detectors placed in the range of scattering angles between 22° and 135°. Such an extended range of scattering angles implies substantial inelasticity effects which were taken into account using Placzek prescriptions. As already discussed [8], it is likely that this correction procedure was used outside the limits of its validity.

The confirmation of the better reliability of the results of Ref. [7] came also from a comparison with simulation results produced with the path-integral Monte Carlo (PIMC) technique. In the investigated thermodynamic region, the agreement between the experimental data and the quantum-mechanical simulation was very good on a quantitative basis [9].

The aim of the present work is to contribute to eliminating the lack of diffraction data on liquid deuterium in the region of the triple point, having in mind also that the knowledge of both the density and the temperature derivative of the static structure factor is of great help in formulating a complete quantum theory of the liquid state, especially in connection with the modeling of the intermolecular correlations [10,11].

In view of the importance of this kind of data we have undertaken a neutron TOF diffraction experiment on deuterium at several thermodynamical states close to the triple point. The reason why deuterium was chosen instead of hydrogen is that for neutron energies larger than 14.6 meV the incoherent molecular cross section of hydrogen is almost two orders of magnitude larger than the coherent one [12]. As a consequence, the coherent-scattering contribution disappears under this overwhelming incoherent background. However, the coherent- and incoherent-scattering cross sections of deuterium are of similar magnitude, and the inelastic-scattering correction for deuterium is smaller than for hydrogen.

This paper reports on the experimental determination of the static structure factor of liquid deuterium in the region of the triple point. The organization of the paper is as follows. In Sec. II we shall describe the details of the experiment, while in Sec. III we will discuss the analysis of the data. The determination of the structure factor and of its density and temperature derivatives will be the subject of Secs. IV and V, respectively, while Sec. VI will be devoted to the comparison of the density derivative with existing theoretical models. The conclusions will be drawn in Sec. VII.

II. EXPERIMENTAL DETAILS

The experiment has been carried out on the Small Angle Neutron Diffractometer for Amorphous and Liquid Samples (SANDALS) at the spallation neutron source ISIS of the Rutherford Appleton Laboratory (RAL), United Kingdom. The measured sample was liquid deuterium at five thermodynamic states in the vicinity of the triple point. The points were selected such that three of them were lying on the 20.7-K isotherm and three on the 25.44-nm^{-3} isochore, as shown in Fig. 1. In this way both the density and the temperature derivatives of the static structure factor could be determined experimentally.

The sample (composed of research-purity deuterium, produced by BDH Chemicals Ltd. and containing hydrogen impurities of less than one part per million) was liquified in a cylindrical vanadium container (11-mm external diameter and 0.2-mm wall thickness), of design similar to the one reported in Fig. 1 of Ref. [7], mounted on the cold finger of a temperature-controlled helium closed-cycle refrigerator. Two temperature sensors,

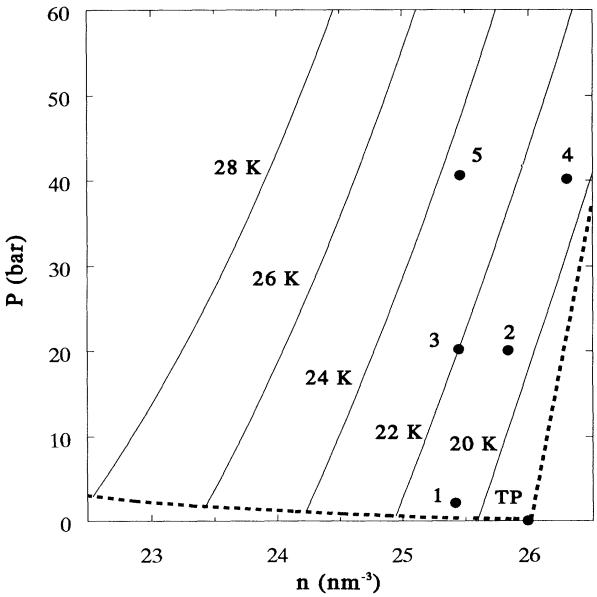

FIG. 1. The thermodynamic coordinates of the experiment as obtained from Ref. [13]. The various states are labeled according to Table II. The dashed lines are the liquid-vapor and liquid-solid coexistence curves.

TABLE II. Thermodynamic parameters of the experiment. The thermodynamic coordinates of the critical point (CP) and of the triple point (TP) are also reported.

State	T (K) [a]	P (bar) [b]	n (nm^{-3})
1	20.7	2.16	25.42±0.06
2	20.7	20.07	25.84±0.06
3	22.0	20.23	25.45±0.07
4	20.7	40.17	26.30±0.05
5	23.5	40.62	25.46±0.07
CP	38.34	16.65	10.435
TP	18.71	0.171	25.99 [c]

[a]The estimated uncertainty in the temperature $\Delta T=0.5$ K which takes into account the measured gradient along the sample container.
[b]The average fluctuation of the measured pressure amounts to $\Delta P=0.1$ bar.
[c]Density of the liquid phase.

made by calibrated Rh-Fe resistance thermometers, were located in the housing of the top and bottom flanges in order to measure both the average temperature and the gradient in the sample. The pressure was measured by means of a calibrated gauge transducer and the molecular number density n was derived by means of the equation of state given by Prydz [13]. The coordinates of the five thermodynamic points are given in Table II. In the following, we will refer to the various thermodynamical states by means of the labels reported in the first column of Table II.

For each thermodynamic point four independent subruns of about 3 h each (equivalent to an integrated proton current of ISIS of 400 μA h) were executed, in order to check both the stability of the sample and of the experimental setup. Moreover, an empty-container run of similar total length as the sample runs was carried out at the beginning and at the end of the experiment, in order to check the long-term stability of the counting electronics and of the instrumental background. The instrumental and sample stabilities were very good, i.e., within the statistical fluctuations of the data.

The TOF diffraction patterns were measured at seven scattering angles, namely, $\theta=9.2°$, 11.8°, 13.1°, 14.6°, 16.2°, 18.1°, and 20.1°.

III. DATA ANALYSIS

In order to perform an accurate inelasticity correction of deuterium diffraction data in the dense phase, the knowledge of the dynamic structure factor $S(Q,\omega)$ in very large Q and ω ranges is required. However, neither experimental results nor reliable models for $S(Q,\omega)$ are available for D_2 in the region of the triple point.

In order to estimate the amount of the inelasticity effects, we have calculated them, at 20.7 K and for the θ values used in the experiment, for a monatomic ideal gas of atomic masses 2 and 4 and with a total neutron scattering cross section σ_s equal to that of the D_2 molecule. For such a system the differential scattering cross section is $d\sigma/d\Omega=\sigma_s/4\pi+P(Q)$, where $P(Q)$ is the contribution of the inelasticity effects.

The results are shown in Fig. 2, where it is seen that $P(Q)$ is large at very small Q but is at most a few percent of $d\sigma/d\Omega$ for $Q>10$ nm^{-1}, and is nearly constant for $Q>40$ nm^{-1}. Based on the assumption that this ideal-gas estimate of $P(Q)$ gives the correct order of magnitude also for the case of deuterium, but is not reliable enough to be effectively applied to the D_2 diffraction data, we have not performed the inelasticity correction. We will reconsider this point, and justify this omission, at the end of this section. It is to be expected, however, that the resulting data for $S(Q)$ will not be accurate at the lowest Q values (i.e., $4<Q<10$ nm^{-1}).

Apart from the inelasticity correction, all the usual corrections for background and container scattering, absorption, multiple scattering, and self-shielding attenuation were performed on the TOF data by means of the available routine package ATLAS [14]; for each scattering angle the final (atom-atom) scattering cross section of D_2 was normalized to absolute units by using the measured diffraction pattern of a vanadium rod of 10 mm diameter which was mounted in place of the sample container in the cryostat. Figure 3 shows the differential cross section $d\sigma/d\Omega$ relative to state 2 for $\theta=20.1°$, as obtained in each of the four independent subruns. The virtual indistinguishability of the four curves from each other, which is found at all θ and for all thermodynamic states of the experiment, shows the good reproducibility of the data taken at a fixed angle. The low-Q region is dominated by the first peak of the intermolecular structure factor, while the oscillations due to the single-molecule form factor

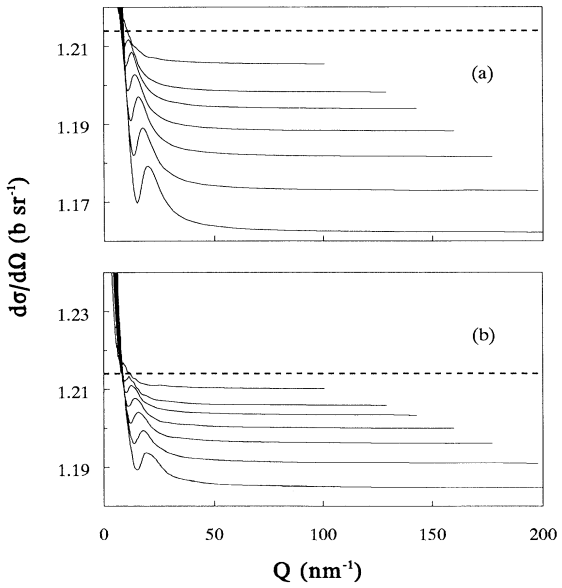

FIG. 2. Differential scattering cross section $d\sigma/d\Omega$ for a monatomic ideal gas of atomic masses 2 (a) and 4 (b), having the same scattering power as the D_2 molecule. The calculation has been performed at $T=20.7$ K for the seven scattering angles of the experiment (θ increases from top to bottom at large Q). The dashed lines are the result for an infinite-mass system [i.e., $\sigma_s/4\pi=2(a_{coh}^2+a_{coh}^2)=1.214$ b sr^{-1}], and the deviations from it represent the amount $P(Q)$ of the inelastic-scattering effects.

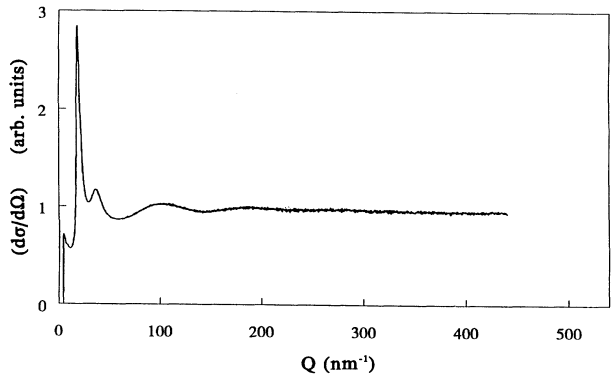

FIG. 3. Differential scattering cross section $d\sigma/d\Omega$ of D_2 at $\theta=20.1°$ for the four different subruns relative to state 2, showing the extremely good stability of the instrumental setup.

characterize the high-Q region.

The differential scattering cross section for a homonuclear diatomic molecule can be written as [15,16]

$$\frac{d\sigma}{d\Omega}=u(Q)[S(Q)-1]+v(Q)+P(Q)\ , \tag{3.1}$$

where $S(Q)$ is the static structure factor of the molecular centers of mass and the functions $u(Q)$ and $v(Q)=v(Q,t=0)$ are molecular form factors which are interpreted as the *intermolecular* and *intramolecular* neutron cross sections respectively. In writing (3.1) the orientational correlations have been neglected, which is a reasonable assumption for D_2 in the present conditions [17].

If a free rigid-rotor model is applied to the molecule, then the expressions for the molecular form factors $u(Q)$ and $v(Q)$ have a very simple analytical form [15]. This model was successfully used in the interpretation of the diffraction data of supercritical deuterium [7]. However, due to the joint effect of the higher density of the present sample (liquid with respect to dense gas) and the much better experimental accuracy achieved with the use of the SANDALS diffractometer [with respect to the liquids and amorphous diffractometer (LAD)], we have found that this simple model was not able to reproduce the present experimental data. The model proposed by Sears [15] was then generalized by assuming that the D_2 molecule in the liquid phase can be modeled as a freely rotating harmonic oscillator [16] and alternative expression for $u(Q)$ and $v(Q)$ were derived, without any further approximation, in form of sequences of functions which converge to the true behavior. For deuterium, it is shown that convergence is achieved after the third iteration [16]. To the lowest-order approximation, the functions are

$$u^{(0)}(Q)=4a_{\rm coh}^2\left[\exp\left[-\frac{\lambda_{\rm DW}^2Q^2}{2}\right]\frac{\sin(QD_e/2)}{(QD_e/2)}\right]^2 \tag{3.2}$$

and

$$v^{(0)}(Q)=2(a_{\rm coh}^2+a_{\rm inc}^2)+2a_{\rm coh}^2\exp(-2\lambda_{\rm DW}^2Q^2)\frac{\sin(QD_e)}{QD_e}\ , \tag{3.3}$$

where $\lambda_{\rm DW}=(\hbar/2M\omega_v)^{1/2}=0.005\,18$ nm is the Debye-Waller length, M, ω_v, and $D_e=0.074\,834$ nm are the molecular mass, the circular frequency of the molecule vibrations, and the average equilibrium distance of the two nuclei, respectively, and $a_{\rm coh}=6.674$ fm and $a_{\rm inc}=4.033$ fm are the coherent- and incoherent-scattering lengths, respectively. It is immediately recognized that Eqs. (3.2) and (3.3) represent the familiar rigid-rotor functions that are now modulated by a Debye-Waller factor. In Ref. [16] it was shown that the functions $u(Q)$ and $v(Q)$ for a freely rotating harmonic oscillator can be well approximated by their zeroth-order iteration provided that the molecular parameters are slightly changed. For example, we find that for deuterium the effective parameters that should be used with our data are $D_e=0.074\,104$ nm and $\lambda_{\rm DW}^2=2.7133\times10^{-5}$ nm^2.

We could now subtract the intramolecular background from the experimental cross section and perform the deconvolution of the molecular form factor. However, this is not straightforward. In fact, the high-Q level of the diffraction pattern did not show the expected monotonic change a function of θ which would be ascribed to inelasticity (see Fig. 2), and was affected by a slightly Q-dependent background. These effects are believed to be due to sample-dependent background in the instrument which introduces systematic errors in the data.

Existing simulation results [18] point out that for $Q>80$ nm^{-1} the intermolecular part of the structure factor vanishes and only the incoherent molecular term $v(Q)$ survives [see Eq. (3.1)]. Therefore, in order to extract the coherent part of the scattering cross section, we have adopted the following procedure. For each scattering angle and each thermodynamic point, we have fitted the data, for $Q>80$ nm^{-1}, to the sum of a parabolic background plus a Q-dependent molecular term:

$$\left[\frac{d\sigma}{d\Omega}\right]_{\rm fit}=A+BQ^2+C\exp(-2\lambda_{\rm DW}^2Q^2)\frac{\sin(QD_e)}{QD_e}\ , \tag{3.4}$$

where the parameters A, B, and C were left free. The molecular parameters, $\lambda_{\rm DW}$ and D_e, were allowed to change only by 1% with respect to their effective values quoted above. The parameter C was left free because this is a measure of the ortho-para composition of the sample [see Eq. (7.8) of Ref. [16]]. As it was expected from a visual inspection of Fig. 3, the resulting value for B turned out to be very small (of the order of 10^{-7} b nm^2). Moreover, since the vanadium container is very poor catalyst for the para-to-ortho conversion, the value of C did not show any trend as a function of time, and its values were always very close (within 1%) to the theoretical value of 0.891 b, which is the computed value for the normal composition. This result is very important because the value of the parameter C represents an *internal calibration* of the amplitude scale and is a confirmation that

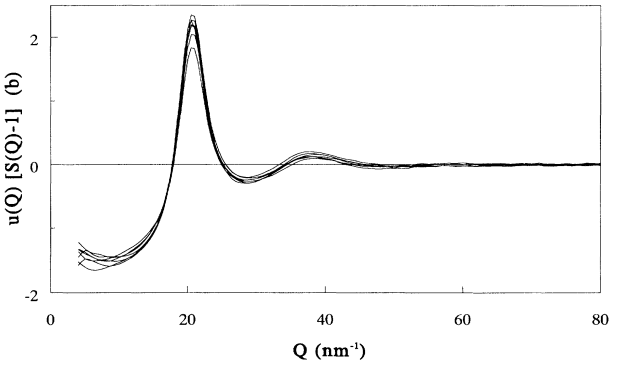

FIG. 4. Coherent differential cross section $u(Q)[S(Q)-1]$ at the seven θ values of the experiment. The spread of the data testifies to the presence of residual systematic errors (see text).

the systematic errors were mainly additive and have been subtracted out, at each scattering angle, in the range of validity of the fit (i.e., $Q > 80$ nm^{-1}).

In order to determine the coherent part of the cross section, we have extrapolated in the low-Q range the incoherent cross section fitted in the high-Q range. Of course we do not expect that for $Q < 80$ nm^{-1} the systematic errors are completely corrected for, but their contribution should have been greatly reduced.

Figure 4 shows seven independent determinations of the intermolecular part of the cross section for state 1. The differences among the determinations from different angles are larger than expected on the basis of the statistical accuracy of the diffraction patterns and do not show any clear dependence on the scattering angle. We attribute this to the presence of residual systematic errors of unknown origin which do not allow, yet, a full exploitation of the instrument's potential. Moreover, these uncertainties are estimated to be of the same order of the inelastic-scattering corrections, which justifies our choice of neglecting them.

Nevertheless, we have been able to obtain seven independent measurements of the same quantity, and therefore an average value and a standard deviation of the coherent contribution to the scattering cross section can be evaluated.

IV. THE STRUCTURE FACTOR

At this point we have derived the experimental results for the center-of-mass structure factor $S(Q)$ and for its thermodynamic derivatives. According to Eqs. (3.1) and (3.2), the coherent diffraction cross section is

$$\left[\frac{d\sigma}{d\Omega}\right]_{\text{coh}} = 4a_{\text{coh}}^2 \left[\exp\left[-\frac{\lambda_{\text{DW}}^2 Q^2}{2}\right]\frac{\sin(QD_e/2)}{QD_e/2}\right]^2 \times [S(Q)-1] , \quad (4.1)$$

from which $S(Q)$ can be obtained. It is worthwhile noting that, in general, the extraction of $S(Q)$ can be performed only in a limited range of Q, because it becomes completely unreliable around the positions of the zeros of the molecular form factor. For deuterium, however, we find a quite favorable situation as the first zero of the form factor is located at $Q \approx 85$ nm^{-1}, where the structure factor has already decayed close to 1.

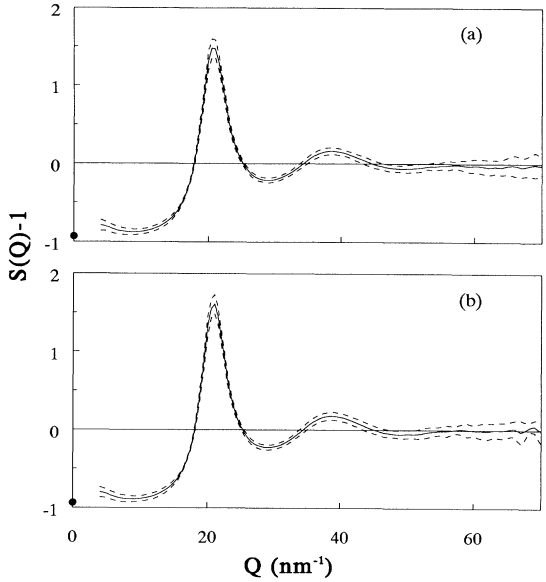

FIG. 5. Center-of-mass $S(Q)$ of liquid D_2. (a) State 1; (b) state 4. The continuous lines are the experimental average values, the dashed lines indicate the limits given by the rms error of seven independent data sets. The values at $Q=0$ (black dots) are obtained from thermodynamic data [13].

The average value of $S(Q)$ is reported in Fig. 5, together with the experimental error interval, for $4 < Q < 70$ nm^{-1}. Figure 5(a) refers to the thermodynamic point 1, which is very close to the triple point, while Fig. 5(b) shows the structure factor relative to the highest density point on the same isotherm (state 4). There is little difference between the two, apart from an expected slight increase in the height of the first peak in Fig. 5(b).

The value at $Q=0$, obtained from thermodynamic data for the isothermal compressibility [13] is also shown in Fig. 5, and appears to be inconsistent with the very-low-Q ($Q < 10$ nm^{-1}) behavior of the structure factor. We have already noted that this is probably due to non-negligible inelastic effects.

V. THE THERMODYNAMIC DERIVATIVES

In evaluating the thermodynamic derivatives of the differential scattering cross section we took advantage of the fact that the intramolecular cross section is independent of n and T and therefore it will cancel out in the numerical differentiation, together with some of the systematic errors and the inelastic-scattering effects, even at $Q < 10$ nm^{-1}. The density derivative at constant temperature of $d\sigma/d\Omega$ has been evaluated at point 2 of the 20.7-K isotherm as the average of the left and right derivatives obtained numerically from the data taken at states 1 and 2, and 2 and 4, respectively, while the temperature derivative at constant density has been evalu-

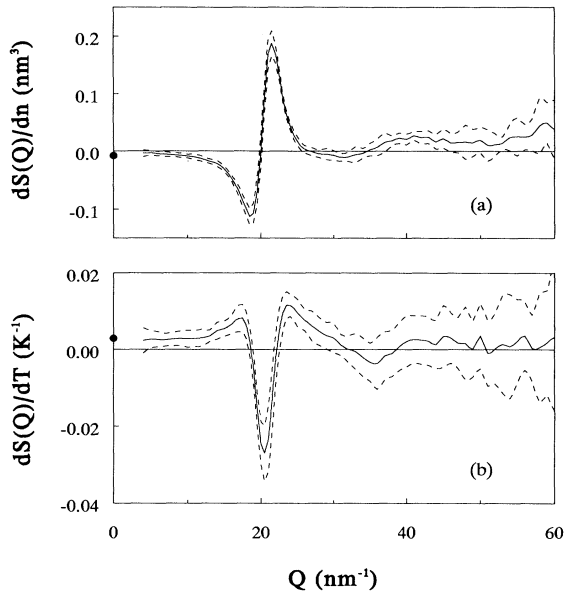

FIG. 6. Average and error of the derivatives of the center of mass $S(Q)$. (a) Density derivative at constant temperature at the thermodynamic state 2; (b) temperature derivative at constant density at the thermodynamic state 3. The values at $Q=0$ (black dots) are obtained from thermodynamic data [13].

ated at point 3 of the 25.44-nm^{-3} isochore by averaging the numerical derivatives obtained from the data at states 1 and 3, and 3 and 5, respectively.

For the density derivative, the agreement among different angles appears to be quite good. However, the differences are slightly larger than expected on the basis of the counting statistics. In any case, the function appears very well defined at low Q and it merges into the noise for $Q>50$ nm^{-1}. A similar result holds for the temperature derivative, apart from larger experimental errors. For both derivatives, but especially for the temperature derivatives, the results at the lowest scattering angle deviate, for unknown reasons, from the common behavior at the other angles.

Equation (4.1) can be used to obtain the thermodynamic derivatives of the structure factor, which are shown in Fig. 6 as averages over six θ values (the lowest angle has been discarded in the average due to the above-mentioned discrepancy), together with their error intervals. The relative errors in the derivatives of $S(Q)$ are larger than those of $S(Q)$ itself, and the amplification of the errors in the high-Q region due to division by the molecular form factor is more evident, especially for the temperature derivative.

VI. MODELS FOR THE DENSITY DERIVATIVE

The density derivative of the static structure factor is an interesting quantity in the theory of simple fluids because it can be related to triplet correlations [10]. The relationship between the pair distribution function $g(r_{12})$ and the triplet correlation function $g_3(r_{12},r_{13},r_{23})$ can be written as

$$\frac{\partial h(r_{12})}{\partial n}=\frac{1}{S(0)}\int\{g_3(r_{12},r_{13},r_{23})-g(r_{12})[1+h(r_{13})+h(r_{23})]\}d\mathbf{r}_3\ , \tag{6.1}$$

where $h(r)=g(r)-1$. Since the Fourier transform of $h(r)$ is $H(Q)=[S(Q)-1]/n$, the experimentally determined $\partial S(Q)/\partial n$ [or equivalently $\partial H(Q)/\partial n$] can be used for testing approximate theories for g_3.

From the formally exact relationship

$$g_3(r_{12},r_{13},r_{23})=g(r_{12})g(r_{13})g(r_{23})\exp[\tau(r_{12},r_{13},r_{23};n)]\ , \tag{6.2}$$

Eq. (6.1) can be written as

$$\frac{\partial h(r_{12})}{\partial n}=\frac{g(r_{12})}{S(0)}\int[h(r_{13})h(r_{23})+g(r_{13})g(r_{23})(\exp\tau-1)]d\mathbf{r}_3\ . \tag{6.3}$$

A density expansion of τ has been used [19,20]:

$$\tau(r_{12},r_{13},r_{23};n)=\sum_{i\geq 1}n^i\delta_{i+3}(r_{12},r_13,r_{23})\ , \tag{6.4}$$

where the coefficients δ_k are sums of cluster integrals over f bonds [$f(r)$ is the Mayer function]. It is found (see Ref. [20] and references therein) that large cancellation effects, present in the evaluation of (6.4), can be reduced to a great extent if one expresses the δ_k's in terms of h-bond cluster integrals. In this way, however, Eq. (6.4) no longer is a true density expansion, due to the implicit density dependence of $h(r)$. Instead, Eq. (6.4) can be recast in the form of a series of products of h functions, whose leading term is of order $O(h^2)$:

$$\tau=n\tau^{(2)}+O(h^3)\ , \tag{6.5}$$

where

$$\tau^{(2)}=\int d\mathbf{r}_4h(r_{14})h(r_{24})h(r_{34})\ . \tag{6.6}$$

Then, to lowest order $O(h^2)$,

$$\frac{\partial h(r_{12})}{\partial n}=\frac{1}{S(0)}\int[h(r_{13})h(r_{23})+n\tau^{(2)}]d\mathbf{r}_3\ , \tag{6.7}$$

whose Fourier transform is

$$\frac{\partial H(Q)}{\partial n}=H^2(Q)\ . \tag{6.8}$$

The approximation (6.8) has been tested on various noble-gas systems [11,20–23].

Another possible approach to the approximation of g_3 is based on the fact that $\tau=0$ corresponds to the Kirkwood superposition approximation [see Eq. (6.2)], so that (6.3) is written as the sum of the Kirkwood term plus a

correction. For $\tau=0$ one obtains

$$\frac{\partial H(Q)}{\partial n}=\frac{1}{S(0)}\left[H^2(Q)+\frac{H(Q)\circ H^2(Q)}{(2\pi)^3}\right], \quad (6.9)$$

where

$$A(Q)\circ B(Q)=\int d\mathbf{Q}'\,A(Q')B(|\mathbf{Q}-\mathbf{Q}'|) \quad (6.10)$$

denotes the convolution of A and B.

The correction to the Kirkwood term is then approximated by means of $\exp(\tau)-1\approx n\tau^{(2)}+O(n^2)$ [see Eq. (6.5)], which contributes to $\partial h(r_{12})/\partial n$ the quantity

$$\frac{g(r_{12})}{S(0)}\int[1+h(r_{13})+h(r_{23})+h(r_{13})h(r_{23})]n\tau^{(2)}d\mathbf{r}_3\ . \quad (6.11)$$

The first term gives, in Q space,

$$\frac{nH(0)}{S(0)}\left[H^2(Q)+\frac{H(Q)\circ H^2(Q)}{(2\pi)^3}\right], \quad (6.12)$$

which adds up to the Kirkwood approximation (6.9) with the result of canceling out the factor $1/S(0)$, so that [24]

$$\frac{\partial H(Q)}{\partial n}=H^2(Q)+\frac{H(Q)\circ H^2(Q)}{(2\pi)^3}+O(n)\ , \quad (6.13)$$

where $O(n)$ denotes terms containing an explicit density dependence.

In Fig. 7 we compare our data for $\partial H(Q)/\partial n$ with the three different approximations (6.8), (6.9), and (6.13) for $g_3(r_{12},r_{13},r_{23})$. As expected, it appears immediately that the simple Kirkwood superposition approximation fails completely in reproducing the experimental behavior. Using Eq. (6.13), instead, brings in a scale factor [$S(0)=0.067$ for state 2, obtained from Ref. [13]] which gives a better qualitative agreement with the experiment, especially in the region of the positive peak ($Q\approx 22$ nm^{-1}). However, the negative peak around $Q\approx 18$ nm^{-1} is not reproduced and a large discrepancy appears at low Q ($Q<10$ nm^{-1}).

The last model we have tested, Eq. (6.8), shows a very similar behavior to the modified Kirkwood expression but avoids the problem of the large discrepancy in the low-Q region. No model for $g_3(r_{12},r_{13},r_{23})$, however, appears to be able to reproduce quantitatively the experimental data and, in particular, the negative peak around $Q\approx 18$ nm^{-1}, and the overall agreement, when present at all, remains at a qualitative level.

A heuristic model which does not involve $g_3(r_{12},r_{13},r_{23})$ was proposed by Egelstaff, Page, and Heard [25] and relates the isothermal derivative of $S(Q)$ to its derivative with respect to Q. In terms of $H(Q)$ the relationship is

$$\frac{\partial H(Q)}{\partial n}=-\frac{1}{n}\left[H(Q)+\frac{Q}{3}\frac{\partial H(Q)}{\partial Q}\right] \quad (6.14)$$

and is based on the hypothesis of a uniformly compressible fluid, i.e., that the intermolecular distances vary as $n^{-1/3}$ when pressure is applied. Approximation (6.14) is also compared with the experimental data in Fig. 7. The agreement is now fairly good on a quantitative basis and the correct size of the two peaks at $Q\approx 18$ nm^{-1} and $Q\approx 22$ nm^{-1} is reproduced.

VII. CONCLUSIONS

The center-of-mass static structure factor $S(Q)$ and its density and temperature derivatives have been experimentally determined in liquid deuterium at thermodynamic states close to the triple point, by means of time-of-flight neutron diffraction. The use of the SANDALS diffractometer at the pulsed source ISIS has ensured very good counting statistics and stability, while the small-angle measurements reduce the amount of inelastic-scattering effects, which are especially important for light-molecular systems. However, the differences among the diffraction patterns taken at different angles are clearly larger than the statistical errors, thus revealing the presence of unknown residual systematic errors. For this reason, inelastic-scattering corrections, which have been estimated to be of the same order as the remaining systematic errors, have not been performed.

We believe, however, that the same problem does not

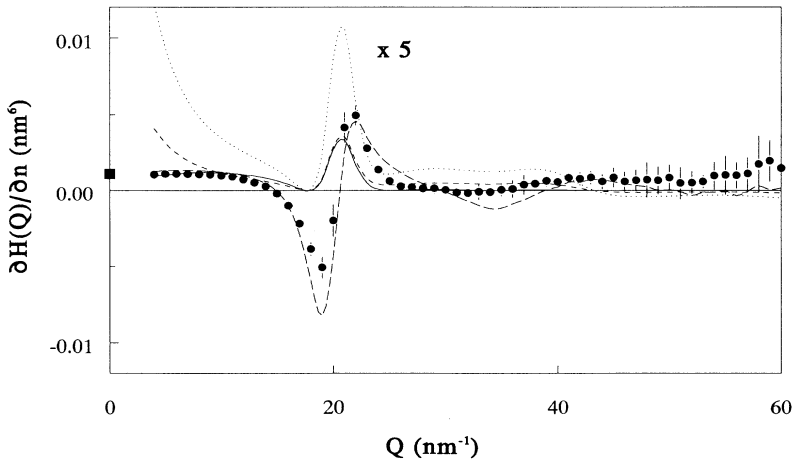

FIG. 7. Density derivative of $H(Q)$. The experimental points (black dots with error bars) are compared with the results of the h^2 approximation (6.8) (solid line), the Kirkwood approximation (6.9) (dotted line), and the modified Kirkwood approximation (6.13) (dashes). The results of the model of Ref. [25], Eq. (6.14), are represented by the long dashes. Note that the Kirkwood approximation results have been reduced in the plot by a factor of 5. The value at $Q=0$ (black square) is obtained from thermodynamic data [13].

affect the determination of the derivatives of the structure factor, because both systematic errors and inelastic corrections cancel out, to a very good approximation, in taking the difference between diffraction patterns at two thermodynamic states close to each other.

The density derivative of $S(Q)$ at constant temperature is related to the form of the triplet correlation function $g_3(r_{12},r_{13},r_{23})$ and has been compared with the expressions derived from some theoretical models for g_3. We note that, although the accuracy of the experimental data is not enough to provide a stringent test of all possible models for $g_3(r_{12},r_{13},r_{23})$, only an order-of-magnitude agreement is found between the present theories and the experiment. Also, we note that a model, which is based on the simple physical hypothesis of a uniformly compressible fluid, gives a remarkably good description of the data, even if no information on the triplet correlations could be extracted.

It is to be remarked that the assumption of a classical fluid underlies all the mentioned theoretical treatments of triplet correlations. A full quantum theory of these microscopic properties does not exist yet, but a numerical evaluation of $g(r)$ has recently become possible by means of the PIMC technique, from which $S(Q)$ and its derivatives could be derived. Such calculations, once available, would allow a quantitative comparison between theory and experiment even for a quantum system such as liquid deuterium. However, no PIMC results are available yet for deuterium in the thermodynamical states of the present study.

It appears, therefore, that more work, both theoretical and experimental, is needed in order to extract reliable information on triplet correlations in low-temperature fluids.

ACKNOWLEDGMENTS

The technical assistance of the ISIS Instrumentation Division of RAL is gratefully acknowledged. This work has been partially supported by GNSM-CNR.

[1] H. R. Glyde and E. C. Svensson, in *Methods of Experimental Physics,* edited by D. L. Price and K. Sköld (Academic, London, 1987), Vol. 23B, Chap. 13, and references therein.

[2] C. Andreani, J. C. Dore, and F. P. Ricci, Rep. Prog. Phys. **54**, 731 (1991).

[3] S. N. Ishmaev, I. P. Sadikov, A. A. Chernyshov, S. L. Isakov, B. A. Vindryaevsky, G. V. Kobelev, V. A. Sukhoparov, and A. S. Telepnev, Zh. Eksp. Teor. Fiz. **94**, 190 (1988) [Sov. Phys. JETP **68**, 1403 (1988)].

[4] J. P. Hansen and I. R. McDonald, *Theory of Simple Liquids* (Academic, London, 1986).

[5] L. A. de Graaf and B. Mozer, J. Chem. Phys. **35**, 4697 (1971); M. C. Bellissent-Funel, U. Buontempo, A. Filabozzi, C. Petrillo, and F. P. Ricci, Phys. Rev. B **45**, 4605 (1992); M. Zoppi, U. Bafile, and R. Magli (unpublished).

[6] G. Placzek, Phys. Rev. **86**, 377 (1952); J. G. Powles, Mol. Phys. **36**, 1161 (1978); **36**, 1181 (1978).

[7] M. Zoppi, R. Magli, W. S. Howells, and A. K. Soper, Phys. Rev. A **39**, 4684 (1989).

[8] M. Zoppi, Physica B **168**, 177 (1991).

[9] M. Neumann and M. Zoppi, Phys. Rev. A **44**, 2474 (1991).

[10] H. J. Raveché and R. D. Mountain, J. Chem. Phys. **53**, 3101 (1970).

[11] D. J. Winfield and P. A. Egelstaff, Can. J. Phys. **51**, 1965 (1973).

[12] J. A. Young and J. U. Koppel, Phys. Rev. A **33**, 603 (1964); K. Carneiro, M. Nielsen, and J. P. McTague, Phys. Rev. Lett. **30**, 481 (1973).

[13] R. Prydz, NBS Report No. 9276, Boulder, CO, 1967 (unpublished).

[14] A. K. Soper, W. S. Howells, and A. C. Hannon, Rutherford Appleton Laboratory Report No. RAL-89-046, 1989 (unpublished).

[15] V. F. Sears, Can. J. Phys. **44**, 1279 (1966).

[16] M. Zoppi, Physica B **183**, 235 (1993).

[17] J. Van Kranendonk, *Solid Hydrogen* (Plenum, New York, 1983).

[18] F. Barocchi, M. Neumann, and M. Zoppi, Phys. Rev. A **36**, 2440 (1987).

[19] R. Abe, Prog. Phys. **21**, 421 (1959).

[20] A. D. J. Haymet, S. A. Rice, and W. G. Madden, J. Chem. Phys. **74**, 3033 (1981).

[21] P. Verkerk, Ph.D. thesis, Technische Hogeschool Delft, 1985 (unpublished); P. Verkerk, J. Phys. (Paris) Colloq. **46**, C9-17 (1985).

[22] P. A. Egelstaff, Annu. Rev. Phys. Chem. **24**, 159 (1973).

[23] W. Montfrooij, L. A. de Graaf, P. J. van den Bosch, A. K. Soper, and W. S. Howells, J. Phys. Condens. Matter **3**, 4089 (1991).

[24] H. Fredrikze, Ph.D. thesis, Technische Hogeschool Delft, 1985 (unpublished).

[25] P. A. Egelstaff, D. I. Page, and C. R. T. Heard, J. Phys. C **4**, 1453 (1981).

[26] R. D. McCarty, J. Phys. Chem. Ref. Data **2**, 923 (1973).

[27] H. M. Roder, G. E. Childs, R. D. McCarty, and P. E. Angerhofer, NBS Technical Note No. 641, 1973 (unpublished).

[28] N. B. Vargaftik, *Handbook of Physical Properties of Liquids and Gases; Pure Substances and Mixtures* (Hemisphere, Washington, D.C., 1975).